Archives of Mechanics • Archiwum Mechaniki Stosowanej • 25, 3, pp. 393–409, Warszawa 1973

# Shock waves in condensing steam flowing through a Laval nozzle

R. PUZYREWSKI, A. GARDZILEWICZ and M. BAGIŃSKA (GDAŃSK)

INVESTIGATIONS of shock waves occurring in a flow of condensing steam are presented. The results of experiments are confronted with a one-dimensional shock wave theory in which the classical surface of discontinuity is replaced by a region of finite thickness named the zone "of intense dissipation".

W pracy przedstawiono badania fal uderzeniowych w kondensującej się parze wodnej. Otrzymane drogą eksperymentu wyniki pomiarów skonfrontowano z jednowymiarową teorią fali uderzeniowej, w której klasyczną powierzchnię ciągłości zastąpiono strefą zwaną tu "strefą silnej dysypacji".

В работе представлены исследования ударных волн в конденсирующемся водяном паре. Полученные путем эксперимента результаты измерений сопоставлены одномерной теории ударной волны, в которой классическая поверхность разрыва заменена зоной называемой здесь „зоной сильной диссипации".

## 1. Notation

$A$ nozzle cross-section area,
$c_p$ specific heat at constant pressure,
$E$ Euler number,
$i$ enthalpy,
$H$ dimensionless parameter,
$h$ heat of condensation and evaporation,
$k$ isentropic exponent,
$L$ nozzle width,
M Mach number,
$R$ gas constant,
Re Reynolds number,
$p$ pressure,
$s$ entropy,
$T, t$ temperature,
$u$ velocity of the mixture of phases,
$X_t$ loss of momentum,
$X$ relative loss of momentum,
$x$ coordinate in the direction of nozzle length,
$y$ nozzle height coordinate, wetness fraction,
$\Delta T$ temperature difference,
$\Delta y$ change of wetness fraction,
$\delta$ boundary layer thickness,
$\varphi$ velocity coefficient,
$\nu$ kinematic viscosity,
$\varrho$ density,
$\theta$ ratio of cross-section areas,

0 refers to stagnation conditions in the medium,
1 refers to conditions ahead of shock wave,
2 refers to conditions down stream of the shock wave,
$\infty$ refers to undisturbed flow,
eks denotes experimental value,
max denotes maximum value,
$s$ refers to saturation state,
$'$ refers to liquid phase,
$''$ refers to gaseous phase.

## 2. Introduction

THE LAVAL nozzle, as a component commonly used in various technical devices, is the object of comprehensive fundamental research aimed at elucidation of the phenomena characteristics of its operation. The flow through the nozzle represents a complex of mutually coupled phenomena, which — in either experimental or theoretical investigations — may be analyzed jointly or separately.

The present work is concerned with investigation into coupled phenomena occurring in the supersonic section of the Laval nozzle, characterized by the presence of shock in the flow of condensing steam. The following phenomena were, in this case, superimposed on the picture observed:

— interaction between shocks and boundary layer (understood as a certain region adjacent to the wall),
— phase changes within the region of wave appearance.

The observations were complemented by measuring static pressures in the relevant region.

The fact of simultaneous occurrence of both the phenomena referred to above makes the experiments somewhat intricate, and also, in the present state of knowledge, makes impossible an elegant and exact theoretical approach. Taking — for example — only the interaction between the shock wave and the boundary layer, we are not able to construct a theoretical description, in spite of the existence of sufficiently developed theories for both phenomena, because of the non-linear effects resulting from their combination.

The investigations presented below were focused mainly on:

— visual effect due to the influence of shock waves on the wetness fraction of condensing steam,
— static pressure disturbances within the region of the shock waves occurrence.

## 3. Conditions of experiments

The experiments were carried out in a symmetric nozzle of rectangular cross-section. The nozzle dimensions and variation of cross-section area along the nozzle axis are shown in Fig. 1. The nozzle inlet conditions were varied within a rather narrow range by throttling or by injecting water into superheated steam. The exhaust pressure was varied by flow throttling in the pipeline leading steam out to the condenser. Thus it was possible to change the location of the shock wave within the supersonic section of the nozzle.

The lines representing isentropic expansion in the "s-i" diagram in the considered interval of condition values are shown in Fig. 2. It may be seen that the initial conditions

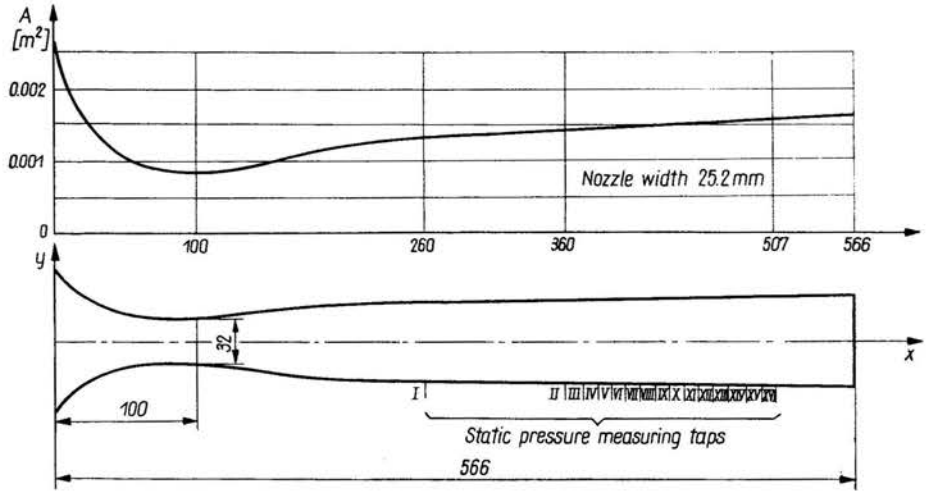


| | | | | | | | |
|---|---|---|---|---|---|---|---|
| x | mm | 0 | 100 | 260 | 360 | 460 | 560 |
| y | mm | 49 | 16 | 26.7 | 28.55 | 30.55 | 32.15 |

FIG. 1.

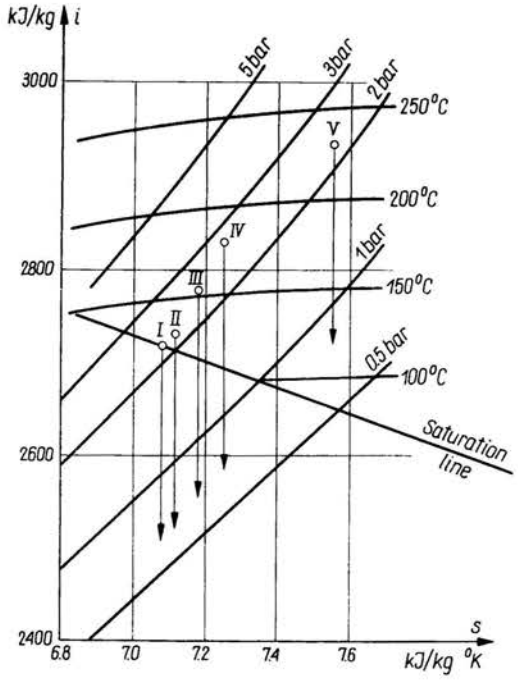


FIG. 2.

were varied from those at saturation line to such corresponding to superheated steam. Visual observations were carried out either with direct lighting, or making use of the Töpler optical system to improve the possibility of indentifying the shock wave. The construction of the nozzle adopted for investigations of this kind has been described, e.g., in [2]. The pressure measurements were made on both side walls of the channel.

## 4. Visual effects caused by shock waves acting on condensing steam

With initial conditions close to the saturation line, the homogeneous condensation starts in the vicinity of the nozzle throat. An appropriate rise of exhaust pressure causes the appearence of a shock wave in the supersonic nozzle section. Due to the increase of steam conditions through the wave, there is a complete evaporation of the condensed water drops. Such a situation is recorded in Fig. 3 with direct lighting, and as it was seen

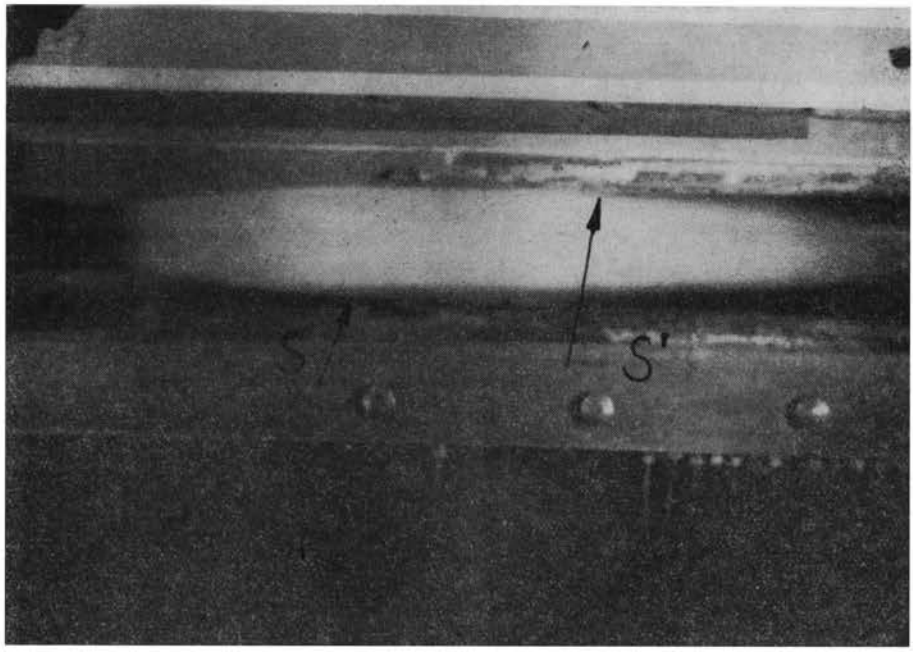


FIG. 3.

with the naked eye. It may be noticed that the liquid phase evaporation path is rather very long. Arrow $s$ gives the probable location of the shock wave. From the growth of the condensationless zone at the wall, clearly visible at the lower wall of the nozzle, it is concluded that there is a flow separation from the wall connected with the wave. The diffuser flow behind the wave carry on to repeated separation of the boundary layer, marked in the photograph with arrow $S'$. This brings about a still stronger compression and rapid evaporation — observable as vanishing of mist in the flow.

With steam conditions $p_0$, $T_0$ over the saturation line, the condensation starts further down from the nozzle throat in the direction of the supersonic section, fig. 4. Drops re-

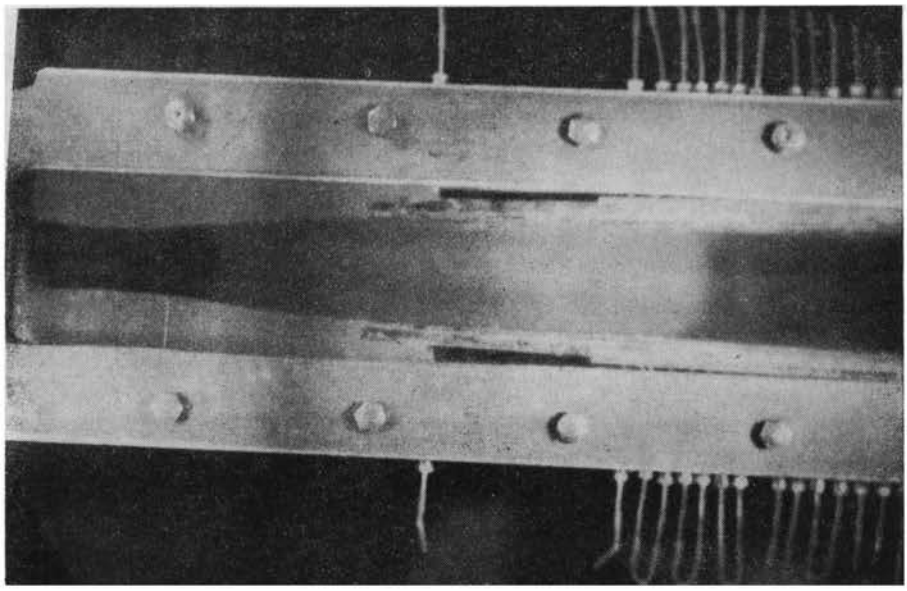

FIG. 4.

sulting from condensation at higher velocities are smaller; they are more sensitive to the change of steam conditions in the wave. Due to the location of the shock waves in the region of higher velocity, the change of parameters is itself larger. Both these causes combine to make shorter than in fig. 3 the path of drop evaporation in the diffuser flow down from the shock.

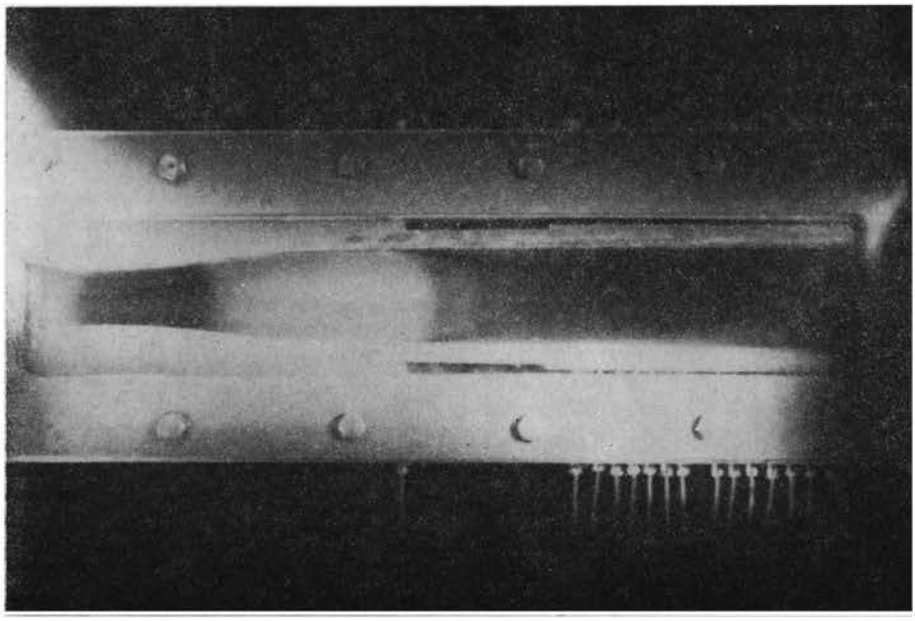

FIG. 5.

A further of rise the initial parameters, together with shifting of the shock wave towards higher velocities, leads to a situation in which the condensation and evaporation occur alternately in a sequence of shock waves, see Fig. 5. Starting from the point of flow separation from the wall (associated with the first shock wave), evaporation and condensation are brought about alternately by secondary expansion due to a change in the effective area of the nozzle cross-section as a result of rapid growth of the boundary layer in the separation zone.

Two or even three succesive shocks may be observed, depending on the location of the first of them. For a record of these waves, obtained by means of the Töpler optical system, see Figs. 6, 7, 8. Somewhat disadvantageous conditions of the Töpler flow visualization must be mentioned. They were caused by vibration of the shocks, and mist due

FIG. 6.

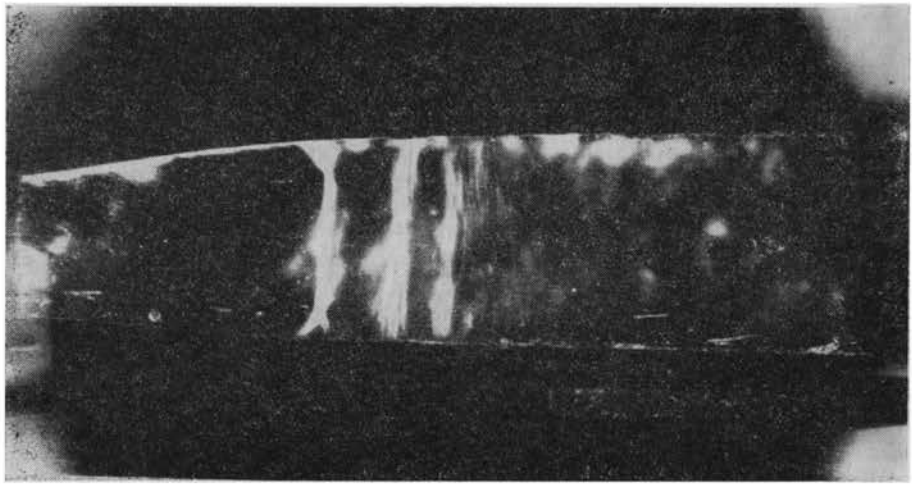

FIG. 7.

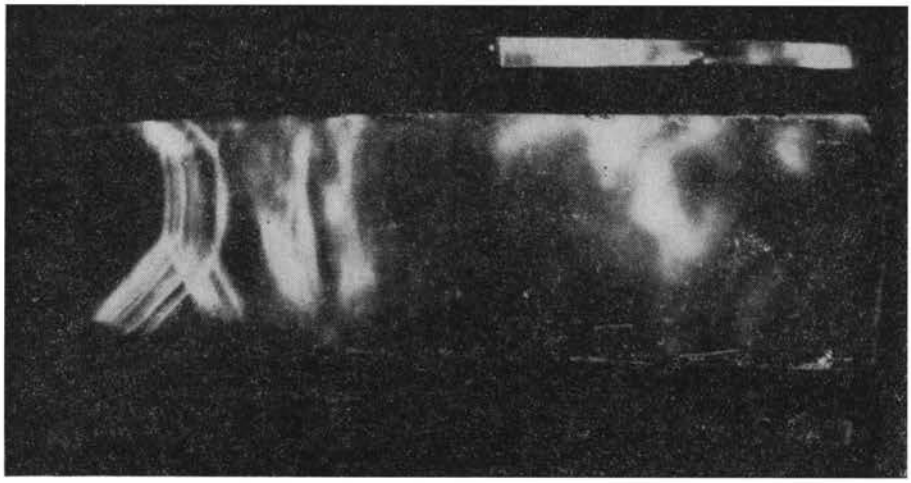

FIG. 8.

to condensation in the flow. The effect of unsteadiness of flow may be seen in Fig. 8, where there are several positions of the first shock observed during exposure. The unclear trace of the shock in Fig. 9 has the same cause. In Figs. 10 and 11, the situation is analogous

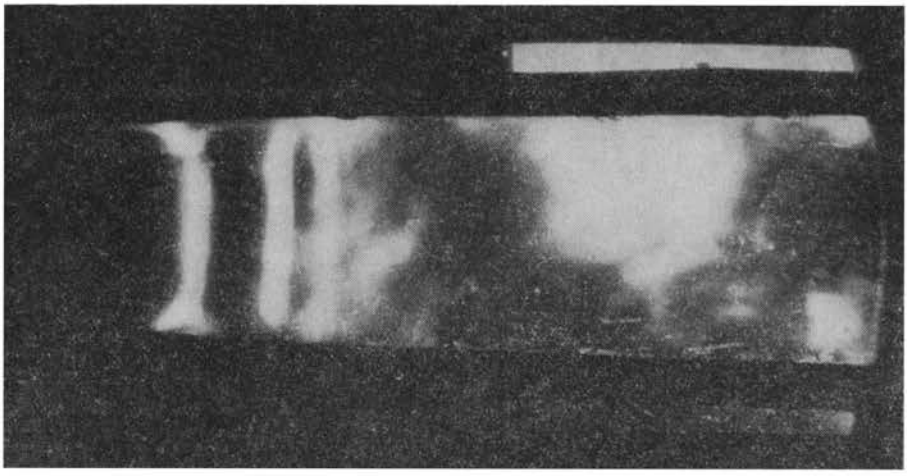

FIG. 9.

to that of Fig. 5. A weak trace of secondary condensation is noticable below the zone of mist evaporation occurring behind the first shock wave.

In Fig. 11, the shocks are situated within the measuring section of the nozzle, relatively far beyond the region of the beginning of condensation. Here, the velocity coefficient, understood as the ratio of local to throat velocities, was about 1.2. The accompanying picture of shocks, taken by means of the Töpler system, is very unclear (cf. Fig. 12). A picture of shock waves in the last figures much more blurred, than those of Figs. 6, 7,

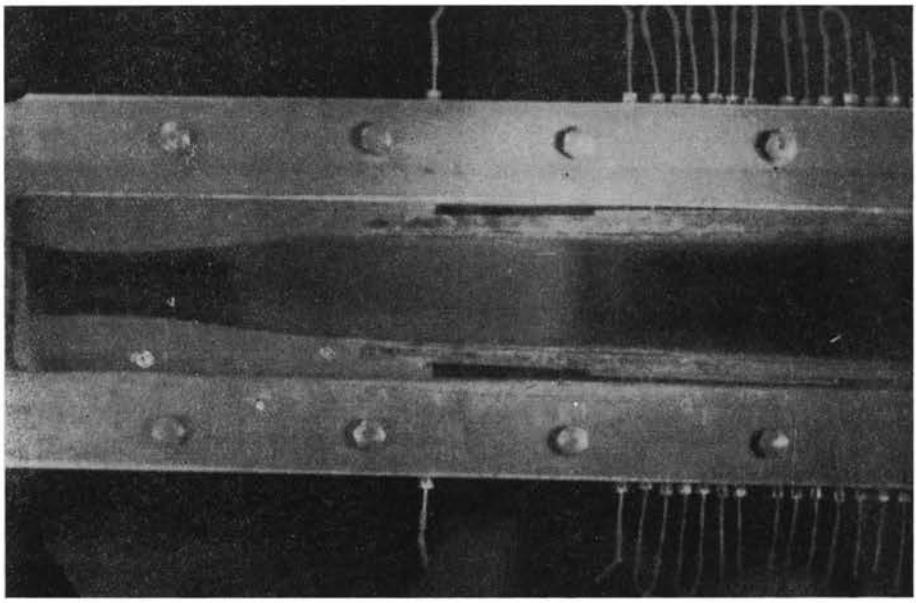

FIG. 10.

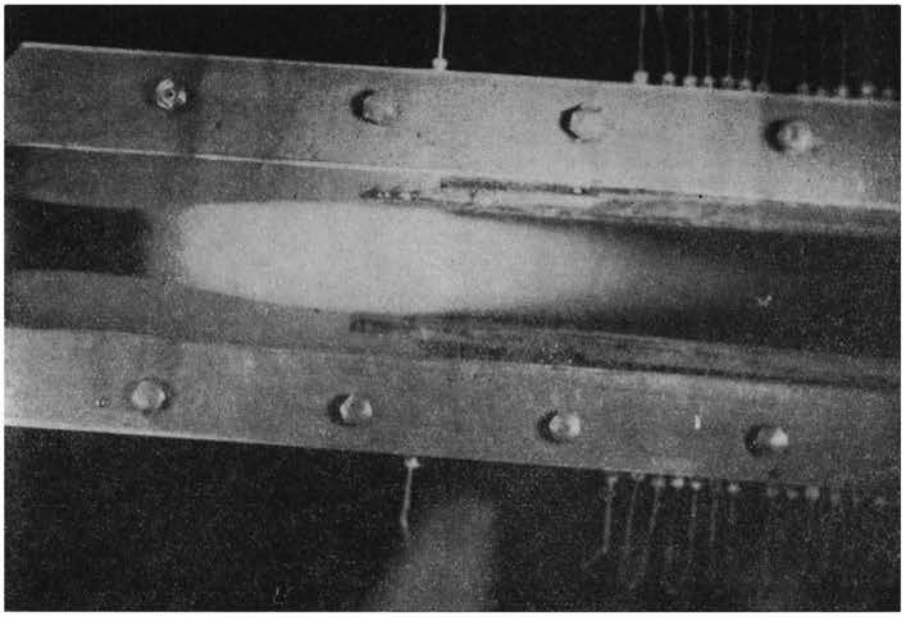

FIG. 11.

and 8 is probably a result of a more distinct influence of evaporating drops on the structure of shock waves in this region. It may be noticed that the shock waves further upstream were not so blurred, because of smaller spacing between the wave and the region of initiation condensation.

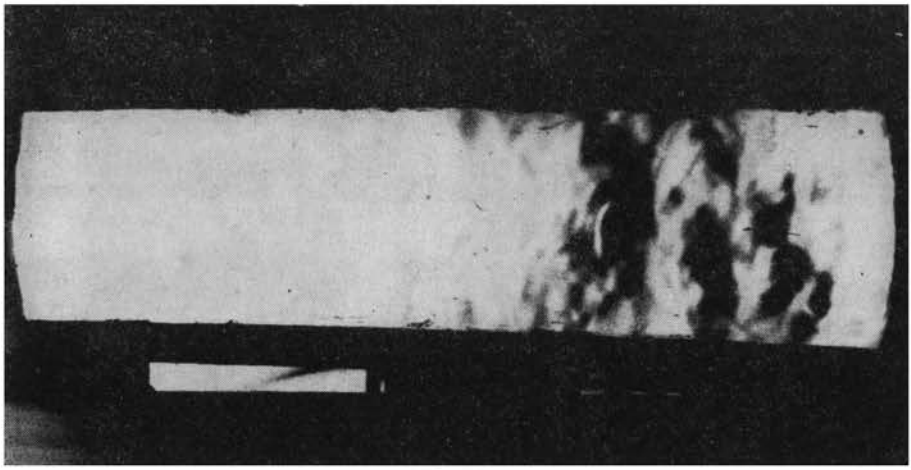

FIG. 12.

The record of phenomena presented above is, for obvious reasons, characteristic for the nozzle shape under consideration. The material presented indicates, however, some characteristic effects of the shock waves and boundary layer on the condensing steam flow in the supersonic section of the Laval nozzle.

An additional observation — outside the program of the measurements — was made during the experiments: rivulets of liquid appeared on the walls of the nozzle supersonic section with large steam wetness at the inlet, cf. Fig. 13.([1])

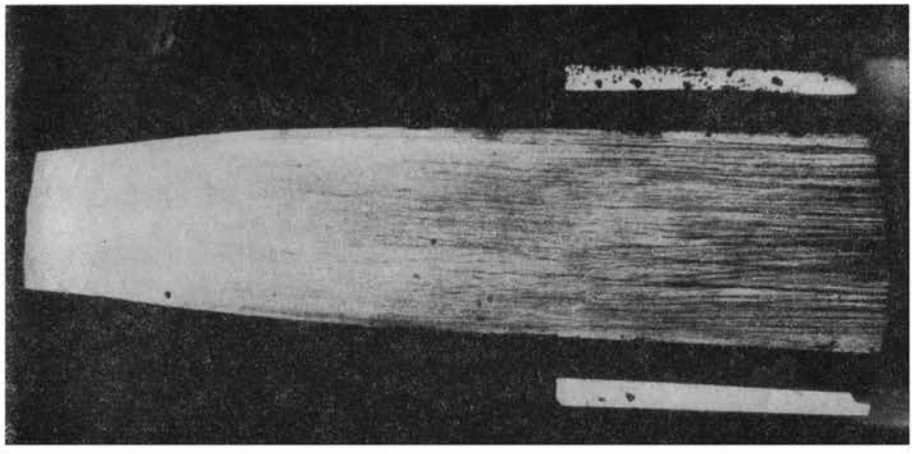

FIG. 13.

In these pictures one can see very clearly the starting points of the dark, thin streams — the water rivulets on the nozzle walls. A uniform, thin water layer cannot be formed because of surface tension on the boundary separating three different phases.

([1]) The $y_0$ value at the inlet was not directly measured. On the basis of data concerning the operating conditions of the test rig, it was estimated at 6 to 8%

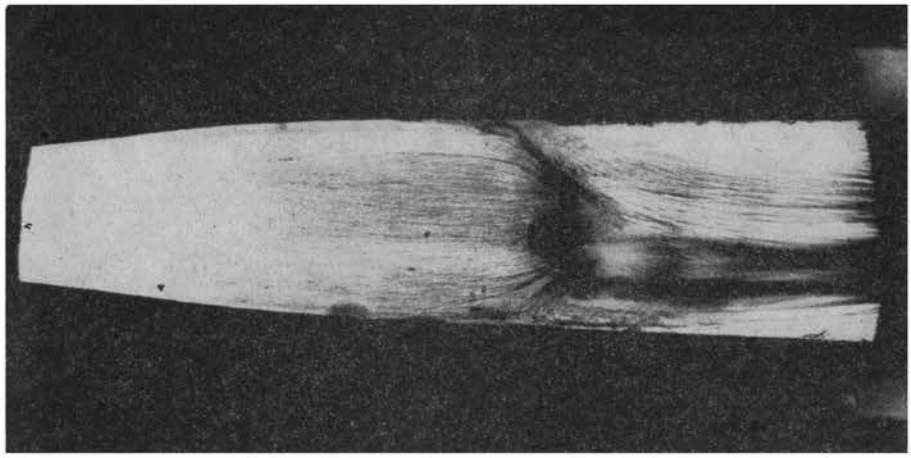

FIG. 14.

The pattern of the paths of rivulets deformed by the shock wave is shown in Fig. 14. The shapes of deformed rivulets enable us to infer separation of the boundary layer from the side walls of the nozzle. On the other hand, vorticity seems to lead to bunching of water rivulets.

## 5. Static pressure disturbances on the nozzle walls in the shock zone

### 5.1. Flow parameters

The pressure disturbances were measured in the situation as in Fig. 11, with shock waves located within the very slightly divergent segment of the nozzle.

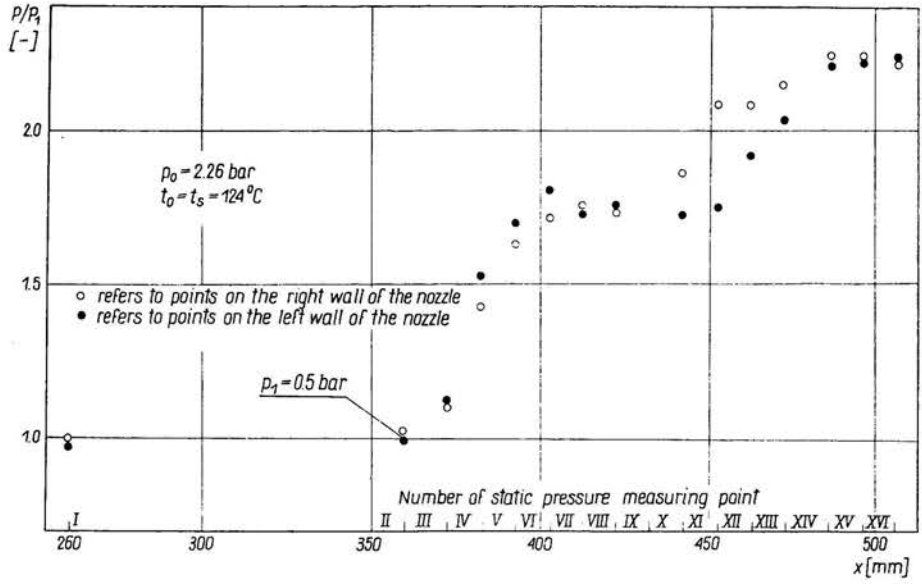


FIG. 15.

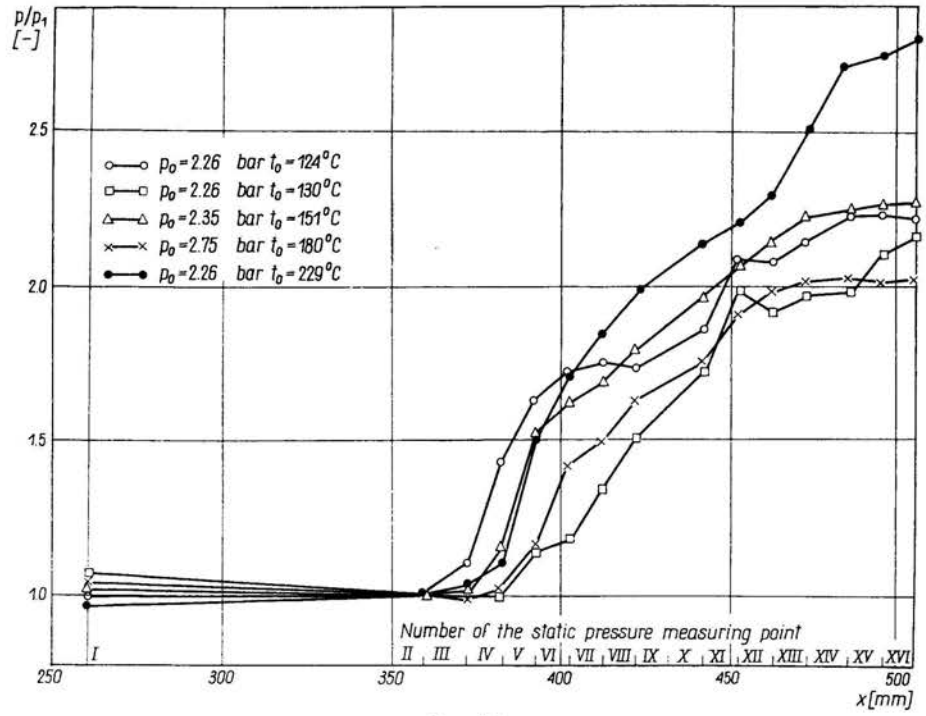


FIG. 16.

The pressure distributions over the nozzle length measured for different sets of experimental conditions listed in Table 1 — are shown in successive Figs. 15 and 16.

The conditions of the sets marked I and II were accompanied by a distinct, strong blurring down stream of the wave system, within the zone of pressure disturbance. In the conditions of set III, a slight mist was observed behind the system of shocks. The conditions of set IV were connected with complete evaporation behind the system of waves. Finally, in the picture corresponding to the Vth set of experimental conditions, there were only very slight traces of mist ahead of the shock wave, disappearing in the shock.

**Table 1**

| Parameters \ Set of experimental conditions | I | II | III | IV | V |
|---|---|---|---|---|---|
| Pressure at nozzle inlet $p_0$ [bar] | 2.26 | 2.26 | 2.35 | 2.75 | 2.26 |
| Temperature at nozzle inlet $T_0$ [cent] | 124 | 130 | 151 | 180 | 229 |
| Pressure at the beginning of the zone of disturbances $p_1$ [bar] | 0.5 | 0.44 | 0.45 | 0.5 | 0.35 |
| Pressure at point of intersection of the isentropic expansion line and the saturation line $p$ [bar] | 2.26 | 2.08 | 1.6 | 1.35 | 0.55 |
| Pressure ratio $p_1/p_0/p/p_1$ | 0.203/4.9 | 0.195/4.7 | 0.191/3.56 | 0.182/2.70 | 0.159/1.57 |

**Table 2**

| Parameters \ Set of experimental conditions | I | II | III | IV | V |
|---|---|---|---|---|---|
| Pressure at the beginning of disturbance zone $p_1$ [bar] | 0.5 | 0.44 | 0.45 | 0.5 | 0.35 |
| Wetness corresponding to thermal equilibrium $y$ [%] | 8.1 | 7.9 | 6.5 | 5.1 | 2.3 |

The Table abowe gives the steam wetness ahead of the shock wave, corresponding to pressure $p_1$, in the instance of isentropic expansion in thermodynamic equilibrium.
The actual wetness may be smaller as a result of supercooling occurring in the expanding wet steam; also, because the expansion is not isentropic.

### 5.2. The intense dissipation zone model

In view of the absence of theories enabling an analytical description of phenomena occurring locally in the shock wave region, a model of a strong dissipation zone was introduced. A considerable positive pressure gradient is assumed for this zone, in contradistinction to the flow of low dissipativity, where the pressure variation is defined by the sequence of cross-section areas and by the losses due to the developed velocity profiles. An idealized picture of pressure variation within the zone, which seems to correspond

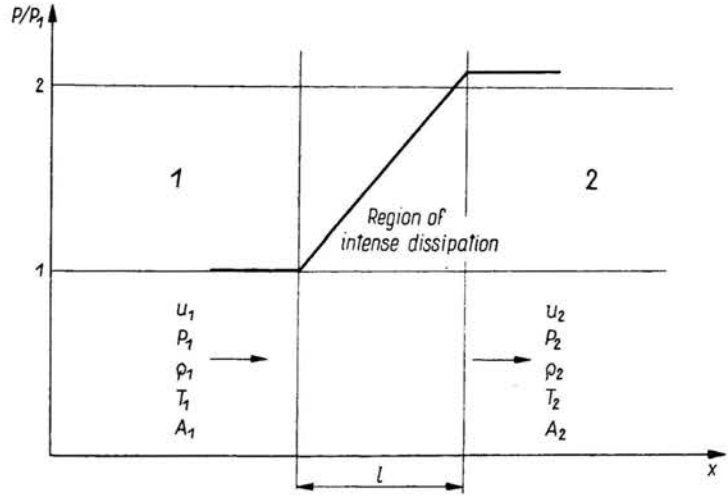


FIG. 17.

to the picture observed experimentally, is shown in Fig. 17. A criterion of applicability of the intense dissipation zone model is the ratio of linear dimensions $2\delta_1/L$; where $\delta_1$ is the conventional boundary layer thickness, and $L$ — nozzle width. It has been proved that there is a strong interaction between the separation region of the shock wave and

the main stream when the ratio indicated is of the order of $10^{-1}$. It leads, then, to the occurrence of a sequence of shocks and to flow separation embracing a considerable region, downstream of which the velocity field becomes "leveled". An estimate of the $2\delta_1/L$ value, based on the thickness of the loss of cross-section area in a turbulent boundary layer on a flat plate ([2])

$$\delta_1 = 0.00153\, H\, (\mathrm{Re})_x^{1/7}\, x$$

yields a value of the order ([3]):

$$2\delta_1/L \approx 0.1$$

The conservation equations for the intense dissipation zone were taken in the one-dimensional form:

$$\frac{\varrho_1''}{1-y_1} u_1 A_1 = \frac{\varrho_2''}{1-y_2} u_2 A_2,$$

$$\frac{\varrho_1''}{1-y_1} u_1^2 A_1 + p_1 A_1 + \int_A p\,dA - X_t = \frac{\varrho_2''}{1-y_2} u_2^2 A_2 + p_2 A_2, \tag{5.1}$$

$$i_1'' - hy_1 + \frac{u_1^2}{2} = i_2'' - hy_2 + \frac{u_2^2}{2}.$$

These were complemented with the equations of state

$$p_1 = RT_1 \varrho_1'', \quad p_2 = RT_2 \varrho_2'', \tag{5.2}$$

and the calorific relation:

$$i_1'' - i_2'' = c_p(T_1 - T_2). \tag{5.3}$$

In addition, the following approximation was made in the relevant region

$$p = p_1 + \frac{A_1 - A}{A_1 - A_2}(p_2 - p_1). \tag{5.4}$$

In the resulting system of equations, the following notation was introduced:

$$E_1 = \frac{RT_1}{u_1^2} \quad \text{(Euler number)},$$

$$H_1 = \frac{hy_1}{u_1^2}, \quad X = \frac{X_t(1-y_1)}{\varrho_1'' u_1^2 A_1}, \quad \theta = \frac{A_2}{A_1}, \quad \varphi = \frac{u_2}{u_1}, \quad \Delta y = y_1 - y_2.$$

The system of equations has the form:

$$-\frac{1}{2}(1-\varphi)^2 + (1-\varphi) = \frac{k}{k-1} E_1 \left[ (1-\Delta y)\theta\varphi \frac{p_2}{p_1} - 1 \right] + H_1 \frac{\Delta y}{y_1},$$

$$(1-\varphi) + \frac{1}{2} E_1 (1-\theta)\,(1-y_1)\left(1 - \frac{p_2}{p_1}\right) = X, \tag{5.5}$$

([2]) $x = 0.4\,\mathrm{m}$, $\nu = 0.4 \cdot 10^{-4}\,\mathrm{m^2/s}$, $u_\infty = 700\,\mathrm{m/s}$. $H = 1.4$, $\mathrm{Re}_x = u_\infty x/\nu$.

([3]) $L = 0.025\,\mathrm{m}$.

with solutions for $\varphi$ or $p_2/p_1$ representing functions of the following parameters:

$$\begin{aligned} \varphi &= \varphi(E_1, H_1, X, \theta, \Delta y, y_1), \\ p_2/p_1 &= \pi(E_1, H_1, X, \theta, \Delta y, y_1). \end{aligned} \tag{5.6}$$

Attention should be drawn to the fact that, for a plain shock, the above functions will be reduced to simple dependences on the Euler or Mach number only, the numbers being mutually related by

$$E = \frac{1}{k\mathrm{M}^2}.$$

In the presence of liquid phase, there is an essential difficulty in determining the sound velocity because of the existence of dispersion, causing the commonly used definition of the Mach number to become meaningless.

The wetness $y_1$ ahead of the dissipation zone is the result of the preceding condensation. There is no full thermodynamic equilibrium during the condensation, and the existing supercooling $\Delta T$ is related to wetness fraction $y_1$ by the function

$$y_1 \cong \frac{c_p}{h}(\Delta T_{\max} - \Delta T), \tag{5.7}$$

where: $\Delta T_{\max}$ corresponds to the maximal supercooling for a given state 1 ahead of the dissipation zone.

The magnitude of supercooling $\Delta T$ is defined by the history of the condensation process from its starting points to the zone of strong dissipation. As proved by the calculations carried out in [2], the values of 1 to 2°C are to be expected in the nozzles.

Some non-isentropic processes are also decisive for the situation referred to as state 1, namely:

(a) losses due to friction of nozzle walls;

(b) changes of entropy associated with condensation. The total entropy increase caused by these factors may be represented as

$$\Delta S = \Delta S_a\left(\mathrm{Re}, \mathrm{M}, \frac{x}{L}\right) + \Delta S_b[\varrho(t), T(t)], \tag{5.8}$$

and the $\Delta S_a$ term may be evaluated using the data from experiments on the Laval nozzles quoted in the literature [3]. The value of $\Delta S_b$ could be assessed only if the run of condensation from initial state 1 were known. However, for determination of the utmost value of $\Delta S_b$, the condensation shock model [4, Figs. 18, 19] may be employed.

With $p_0$, $T_0$ and the values of $p_1$, $T_1$ and $S$ being given, the state 1 ahead of the dissipation zone is known. All the values of parameters taking subscript 1 are, therefore, determined. Only the values of $\theta$, $X$, $\Delta y$ are still to be determined. But here, the information supplied by the investigations is only fragmentary. The value of $\theta$ for the dissipation zone was determined from the sequence of nozzle cross-section areas, static pressure distribution and the zone width established on the basis of Fig. 16.

The function $(5.6)_2$

$$p_2/p_1 = \pi\left(X, \frac{\Delta y}{y_1}\right)$$

was calculated for a selected set of stagnation parameters marked with subscript 0 and the parameters ahead of the dissipation zone — subscript 1.

The run of this function is shown in Fig. 18. The curve of Fig. 18 was employed to determine the $X = X(\Delta y)$ dependence for $p_2/p_1$ values observed during the experiments.

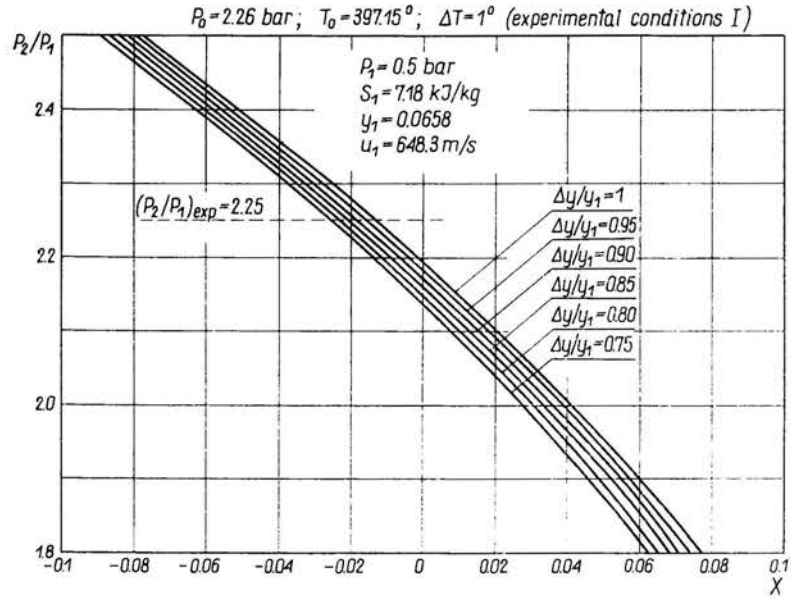


FIG. 18.

There is one link missing in the reasoning leading to the determination of the loss of momentum referred to the momentum of the flow ahead of the dissipation zone: the change of the wetness fraction $\Delta y/y_1$. This ambiguity cannot be removed by way of a formalism based on the conditions of conformity.

The course of variation of the $X = X(\Delta y/y_1)$ dependence for four sets of conditions ahead of the dissipation zone is shown in Fig. 19. The same figure contains, in addition, a graph of quantity $\Delta T(p_2) = T_2 - T_s(p_2)$ characteristic of the superheating of steam in state 2 for the sets of experimental conditions in which the phenomenon of superheating is formally possible.

Attention should be drawn to the fact that, for values below unity, a wetness is obtained in the region of superheated steam. This would mean physically, that the time of evaporation of drops is longer than the time of their passage through the intense dissipation zone.

There is a point marked in fig. 19 corresponding to the solution for the V-th set of conditions on the assumption of $\Delta T = 1°C$ supercooling. In this instance, the characteristic plotted in the reference frame adopted reduces itself to a point, as a consequence of complete evaporation.

Some comments should be made on the negative value of $X_t$ — coefficient obtained from the calculations. This would indicate the existence of a force acting in the direction

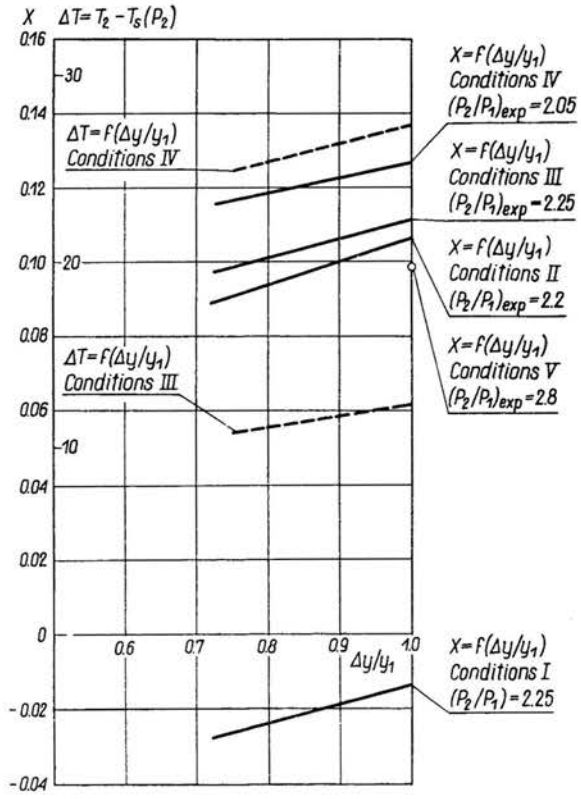


FIG. 19.

of flow. The error analysis carried out by the authors shows that this result is not explicable as an error in calculation or measurement. A convincing explanation is hardly possible without knowledge, also, of the structure of the intense dissipation zone.

A possible formal reason may be sought in the non-uniformity of the field of parameters. It seems, however, that the adoption of the one-dimensional model should not lead to excessive errors if the cross-sections upstream and downstream of the zone manifest a fairly "good" ordering of the parameters. Another possible source of this result may be sought in the components of the stress tensor appearing in the equation of motion for the two-phase fluid [5]. Here, the situation in the neighbourhood of the wall may, in view of the possible occurrence of reverse flows, be of importance in the interpretation.

## 6. Conclusions

Observations of shock waves in the condensation region of the flow of steam through a Laval nozzle constitute the main results of the present work.

The formalism adopted and commonly used for shock waves, and complemented with the concept of the intense dissipation zone, appeared to be not entirely successful as regards information on the change of steam parameters across the zone. This may

be ascribed to the intricacy of the phenomena occurring in the region under consideration. The process of phase changes is, in the first place, non-definable within the framework of the approach suggested. The duration of these processes plays an important part in such an analysis.

A comparison between the calculations and the results of pressure measurement enables estimation of the order of magnitude of the losses of momentum within the zone of intense dissipation.

Comparing the calculated and measured values with the results obtained in [1], we may infer that the coefficient $X = X\,(1-y_1)/\varrho_1'' u_1 A_1$ has no conservation properties. On the other hand, it depends markedly on the channel geometry, moisture content and on the picture of phenomena in the dissipation zone.

The formation of the rivulets of liquid on the nozzle walls is an interesting physical phenomenon. It may result from the transport of drops to the walls combined with the effect of surface tension on the interface of three phases the surface tension not allowing an uniform liquid film to form. It is also possible that this form of liquid is a product of condensation on the walls. Some data concerning wall temperature is indispensable to a better insight into this problem.

## 7. References

1. R. PUZYREWSKI, M. BAGIŃSKA, A. GARDZILEWICZ, *Zmiany ciśnienia statycznego w obszarze występowania fali uderzeniowej w kondensującej się parze wodnej w dyszy de Lavala* [Static pressure variation in the shock region, in condensing steam flowing through a Lavel nozzle; in Polish], Prace IMP PAN, Fasc. 57, 1971.
2. R. PUZYREWSKI, *Kondensacja pary wodnej w dyszy de Lavala* [Steam condensation in a Laval nozzle, in Polish], PWN, Warszawa-Poznań 1969.
3. М. Дейч, Г. Филиппов [M. Dejcz, G. Filippow], *Газодинамика двухфазных сред* [Gas dynamics of two-phase media, in Russian], *Энергия*, Moscow 1968.
4. R. PUZYREWSKI, A. GARDZILEWICZ, *Niektóre wyniki badań przepływu pary wodnej z kondensacją przez dysze* [Some results of experiments on condensing steam flow through nozzles, in Polish], Prace IMP PAN, Fasc. 25, 1965.
5. R. PUZYREWSKI, T. JANKOWSKI, *Równania zachowania dla ośrodka dwufazowego* [Conservation equations for two-phase media; in Polish], Prace IMP PAN, Fasc. 50, 1970.

INSTITUTE OF FLUID FLOW MACHINERY IN GDAŃSK

*Received December* 14, 1971